Investigation on the Relationship Between Normal Incidence and Random Incidence Sound Transmission Loss

Sheng Gu[1,2], Ziyang Wang[2,*] and Hequn Min[2]

[1]Kunshan Construction Engineering Quality Testing Center Co., Ltd., Kunshan, Jiangsu, 215300, China
[2]Key Laboratory of Urban and Architectural Heritage Conservation, Southeast University, Nanjing, Jiangsu, 210096, China

*Corresponding author's e-mail: wangziyang@seu.edu.cn

Abstract. The objective of this study is to examine the relationship between the normal incidence sound transmission loss and the random incidence sound transmission loss of diverse configurations of finite large plates. Firstly, theoretical analyses and simulation models are applied to analyze the sound insulation performance of single-layer and multi-layer panels, utilizing the Equivalent Single Layer method and the Layer-Wise method. The impact of the dimensionless participation factor on the sound transmission loss is examined in depth. Finally, the relationship between the normal incidence and random incidence sound transmission loss of different configurations is discussed in the context of stiffness control and quality control. The findings indicate that when the participation factor of the plate remains constant, the sound transmission loss discrepancy exhibits a comparable alteration pattern. In the stiffness control area, the sound transmission loss disparity among diverse configurations can be approximated as 0 dB. Within the scope of quality control, the theoretical formula is applicable to the plates with a straightforward configuration, whereas for complex configurations, the formula offers a general indication of the trend.

Keywords: Architectural sound insulation; Normal incidence sound transmission loss; Random incidence sound transmission loss

1 Introduction

The sound insulation performance of a building is an important criterion for evaluating its overall quality. The most frequently used techniques for measuring sound transmission loss (STL) of components are the reverberation chamber method [1] and the standing wave tube method [2]. It is possible to reduce expenditure significantly if the results of simple normal incidence sound insulation performance measurements can be applied to estimate the random incidence sound insulation performance closer to the actual use case.

W. He et al. (eds.), *Proceedings of the 2024 10th International Conference on Advances in Energy Resources and Environment Engineering (ICAESEE 2024)*, Atlantis Highlights in Engineering 36,
https://doi.org/10.2991/978-94-6463-708-3_19

At present, there have been many related studies for the sound insulation performance of panels. Analytical methods [3,4] are often used for simple configurations. With the development of computer technology, numerical methods such as finite element method (FEM) are widely used to study the sound insulation performance of complex panels. D'Ottavio et al. [5] introduced a simplified modeling method (sub-LW method) for multi-layer panels. Wang et al. [6] proposed a high-order sub-LW computational model of acoustic-solid coupling that considers both computational accuracy and efficiency. Zhang et al. [7] proposed a semi-analytical vibroacoustic model for viscoelastically damped composite laminates. Li et al. [8] numerically investigated the vibroacoustic response and STL of adjustable Poisson's ratio sandwich panels in hot and humid environments.

However, there is a paucity of studies examining the relationship between random and normal incidence sound insulation performance. At present, the value of the normal incidence STL minus 5.5 dB is frequently employed to estimate the random incidence STL for the 1/3 octave band in engineering [9]. This method is based on the assumption of Sharp's infinite plate and is applicable to the mass law control range. Mahjoob et al. [10] developed an asymptotic impedance model to predict the normal incidence STL for a three-layer panel containing Newtonian fluid. They also sought to arrive at the random incidence STL by correcting this value. However, the discrepancy between the predicted and experimental results is considerable.

In this paper, a numerical analysis model is established utilizing the sub-LW method to carry out theoretical analysis and simulation studies on the STL of a finite large plate in the low and medium frequency bands. The simulation results are compared with the published computational data to verify the accuracy of the simulation model. The influence of the dimensionless participation factor on STL differences is thoroughly examined, along with an analysis of the relationship between random and normal incidence STL by using a number of examples with different configurations in the stiffness controlled and quality controlled areas, respectively.

2 Theory Analysis

2.1 Theoretical Formula for Sound Transmission Loss

This section presents a prediction equation for the difference in STL within the quality control area for plates of the same size, based on previous research. For an infinitely large plate, the normal incidence STL can be described by the mass law expression as follows:

$$STL_n = 10\lg\left(1 + \frac{\pi f m}{\rho_0 c}\right). \tag{1}$$

Under diffuse sound field excitation, the transmission coefficient can be described as follows:

$$\tau = \frac{1}{\pi}\int_0^{\frac{\pi}{2}} d\theta \int_0^{2\pi} \tau(\theta,\varphi)\sin\theta\cos\theta d\varphi. \tag{2}$$

In the quality control area, the transmission coefficient of the plate under forced vibration for random incidence can be expressed as: [4]:

$$\tau_r \approx \frac{\tau_{nr}}{200\left(\frac{A}{P\lambda_C}\right)^2 \eta} = \frac{\tau_{nr}}{200\left(\frac{Af_C}{PC}\right)^2 \eta}, \tag{3}$$

where f_c is the critical frequency; ᴧ and A are the plate's surface area and the length-to-edge ratios, in that order.

Collation yields a prediction equation for the disparity in random and normal incidence STL of a single-layer square plate, as follows:

$$\begin{aligned} \Delta STL = STL_n - STL = 10\lg(1+\frac{\pi fm}{\rho_0 c}) - 20\lg\left[\frac{\pi fm(f_c^2 - f^2)}{\rho_0 c f_c^2}\right] \\ +10\lg\left[\ln(\frac{2\pi f\sqrt{ab}}{c}) + 0.16 + \frac{c^2 ab}{16\pi^2 f^2} - U(\Lambda)\right] + 10\lg\left[\frac{1}{2} + \frac{c^2(a+b)^2}{100\eta(abf_c)^2}\right]. \end{aligned} \tag{4}$$

2.2 Numerical Analysis Model

As depicted in Figure 1, imagine a oblong panel (the midline of the plate is taken as the longitudinal coordinate origin) positioned within an endless solid barrier, where various boundary conditions can be selected as required. The panel transmits incident sound waves from one side to the opposite side.

When a planar sound wave is incident at an angle to the surface of the specimen, the planar acoustic wave can be represented by:

$$p_i(x,y,z) = \widehat{P}_i \exp\left[-\mathrm{i}\left(k_x x + k_y y + k_z z\right)\right]. \tag{5}$$

When considering a scattered sound field caused by random incidence, the acoustic wave can be represented as follows:

$$p_i(x,y,z) = \widehat{P}_i \frac{1}{\sqrt{N}} \sum_{n=1}^{N} \exp\left[-\mathrm{i}\left(k_{xn} x + k_{yn} y + k_{zn} z\right)\right]. \tag{6}$$

The sound insulation performance of the panel structure under consideration in this study is defined in terms of STL, which is expressed as

$$\mathrm{STL} = 10\log\left(\frac{W_i}{W_r}\right), \tag{7}$$

where W_i and W_r denote the incident and transmitted acoustic energy. The energy of the incident sound wave can be expressed as follows

$$W_i(\theta,\varphi)=\frac{\left|p_i\right|^2 S\cos\theta}{2\rho_0 c}, \tag{8}$$

where S and $\rho_0 c$ represent the structural surface area and characteristic impedance of air, respectively.

The incident acoustic energy can be expressed as:

$$W_r(\theta,\varphi)=\frac{1}{2}\int_{\Sigma_{SA}}\Re(\hat{p}_r v_n^*)d\sum_{SA}=\frac{S_e}{4}\Re\left\langle \mathbf{v}_n^H\left(\mathbf{Z}^H\mathbf{Z}\right)\mathbf{v}_n\right\rangle=\mathbf{v}_n^H\mathbf{R}\mathbf{v}_n, \tag{9}$$

where the superscripts * and H denote the complex conjugate and Hermitian transpose, respectively; v_n are the complex normal velocity amplitudes; $\hat{p}_r$ represents the sound pressure; S_e denotes the surface area of each simulation cell; $\boldsymbol{R}$ represents the real component of the radiating impedance matrix.

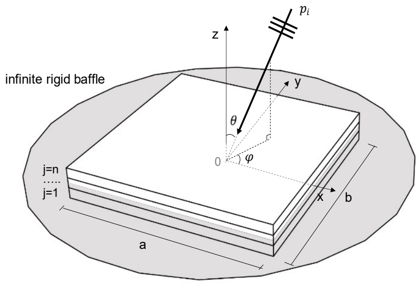

Fig. 1. Schematic diagram of the model.

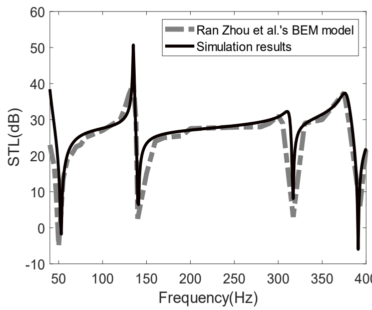

Fig. 2. Reproduction of model results.

2.3 Validation of FEM Models

FEM models are utilized in COMSOL Multiphysics software to numerically compute the STL variations of different structures under various acoustic wave excitations. In order to maintain the accuracy of numerical computation results, the discretization process (i.e., the meshing operation in the software) must maintain mesh density, meeting the minimum and maximum size criteria. This part presents a validation of the established finite element numerical analysis model using experimental results from the literature.

Figure 2. shows the calculated results of FEM compared with the normal incidence STL results from the numerical simulation results of Zhou et al. [11]. This analysis focuses on an AL plate, which is supported on all four edges. The dimensions of the plate are 0.84m by 0.428m, with a thickness of 3.175 mm, and the material properties are shown in Table 1.In the frequency band of the study, the trend of the STL is

basically the same with good consistency and the modal eigenfrequencies obtained by the computational model in this paper accurately coincide with the simulation results of Zhou et al.

Table 1. Properties of materials used in the study.

Material	ρ(kg/m³)	Poisson ratio γ	Young's modulus E (GPa)	η(%)
AL	2700	0.33	70	0.01
Fiberboard	880	0.15	3.5	0.02
Plasterboard	760	0.24	2.1	0.02

3 Results and Discussions

This section provides an analysis of the sound insulation characteristics of a finite-sized plate under solidly supported boundary conditions, with particular consideration of the influencing factors. This is achieved through the use of a finite element computational model. Additionally, the relationship between random and normal incidence STL in the stiffness control area and the quality control area of different configurations of the investigated test plate is also discussed based on the simulation results. Among which, Table 1 lists the comprehensive material properties.

3.1 Discussion on Dimensionless Participation Factors

Throughout this segment, the participation factor [12] is invoked to investigate the relationship between physical parameters such as specimen size and thickness and the STL characteristics of the test plate:

$$\phi = \frac{ab\eta^e}{h^2}, \tag{10}$$

where η^e represents the effective loss factor.

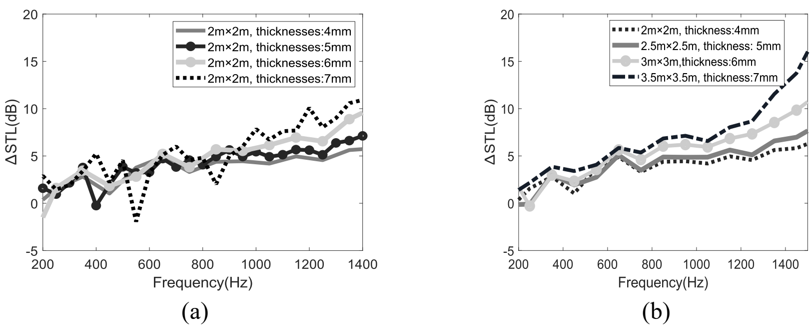

Fig. 3. Variations in STL for plates of different constructions. (a) All plates measure 2m × 2m; (b) Participation factor=5000.

Figure 3(a) depicts a test plate with dimensions of 2m × 2m, wherein the varying thicknesses of the test plates are associated with distinct participation factors. In contrast, Figure 3(b) illustrates a random incidence plate with varying thicknesses, exhibiting a uniform participation factor achieved through the manipulation of the plate's surface dimensions. A comparison of the two figures reveals that the panels have the same dimensionless factor and that the trend of STL differences is similar. Based on the findings of this study, within the quality control area, an expression can be proposed to estimate the STL difference when both random and normal incidence of the plate are controlled.

3.2 Analysis of Stiffness Control Area Results

Figure 4 presents a comparison of the random incidence STL curves with the normal incidence STL curves for different configurations of test panels (single-layer, sandwich) under solidly supported boundary conditions. The dimensions of the panels under investigation are all 0.2 m × 0.2 m. The random incidence STL curves for single-layer aluminium panels were obtained through numerical integration of the results of the angles using Equation (2) and through the finite element simulation model. The results of these two methods were in good agreement with one another. The results demonstrate that the discrepancy in STL between the four distinct plate configurations examined within the stiffness control area is nearly negligible, with a difference of approximately 0 dB.

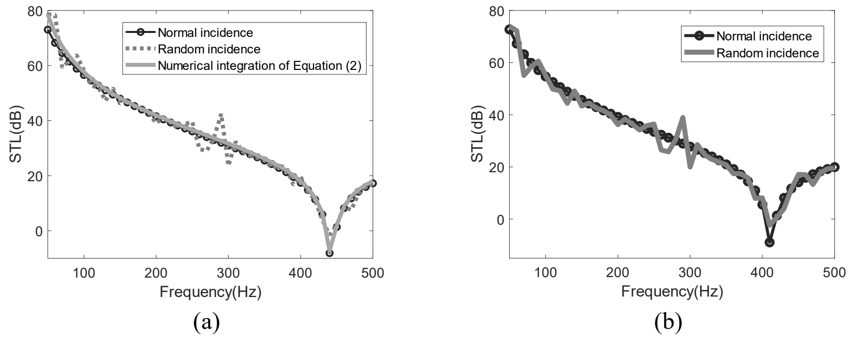

Fig. 4. STL for different configurations of plates in the stiffness control area. (a) 2mm thick AL plate; (b) 2mm plasterboard + 2mm fiberboard + 2mm plasterboard.

3.3 Analysis of Quality Control Area Results

Figure 5(a) shows a juxtaposition of the simulated results with the predicted curves of the STL difference for varying sizes of single-layer aluminium panels (test panel 1: 2m×2m, 2mm; test panel 2: 3m×3m, 6mm) with solidly-supported boundary conditions. Figure 5(b) illustrates the simulated and predicted curves for the sandwich panels with the same boundary conditions. The sandwich panels comprised fibreboard bonded to the upper and lower gypsum boards (test panel 3: 2mm+1mm+2mm, test panel 4: 2mm+2mm+2mm). In the case of the sandwich boards, the difference in STL was approximated using the Equivalent Single Layer method. A comparison of the data indicates that the prediction results are in good agreement with the simulation results. Furthermore, the estimation formula for the quality control area is found to have good accuracy and applicability.

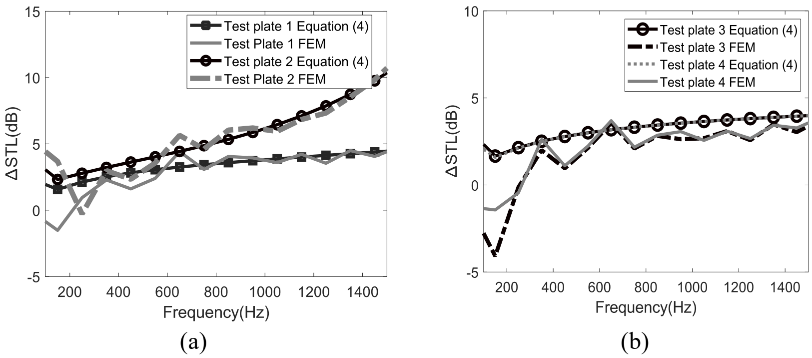

Fig. 5. STL differences among various plate configurations within the quality control area. (a) Comparisons for single-layer panels; (b) Comparisons for sandwich boards.

4 Conclusions

In this paper, the relationship between the STL at random and normal incidence for a finite large plate is discussed. The influence of the dimensionless participation factor on the STL is investigated through the development of a finite element computational model. Furthermore, the discrepancy in STL between stiffness control and quality control area is also estimated based on previous research.

The research indicates that the difference in STL can be approximated to 0 dB for various configurations of the examined panels in the stiffness control area. Similarly, panels with the same participation factor in the quality control area exhibit a comparable trend. This can be derived using the prediction formulae for panels with simple structures and fewer layers. Furthermore, the formulae provide insights into trends for more complex configurations. This study offers methodological backing for the simple evaluation of building insulation capabilities in components and presents a straightforward tool for predicting the random incidence STL of finite, large rectangular panels in both the stiffness and quality control areas. This is highly significant for enhancing occupant comfort in buildings and improving inspection efficiency.

Acknowledgments

This work is supported by the project 'Research on Rapid Measurement Methods for Sound Insulation Performance of Building Walls Using Small-Scale Component

Testing in Field Applications', funded by Kunshan Construction Engineering Quality Testing Center Co., Ltd.

Reference

1. ISO, Acoustics - Laboratory measurement of sound insulation of building elements, Standard 10140-5: 2010, International Organization for Standardization.
2. ISO, Acoustics - Determination of sound absorption coefficient and impedance in impedance tubes, Standard 10534-2: 1998, International Organization for Standardization.
3. Cremer L (1942) Theorie der schalldämmung dünner wände bei schrägem einfall. Akustische Z. 7: 81-102.
4. Sewell E C (1970) Transmission of reverberant sound through a single-leaf partition surrounded by an infinite rigid baffle. J. Sound Vib., 12: 21-32. [https://doi.org/10.1016/0022-460X(70)90046-5].
5. D'Ottavio M (2016) Sublaminate Generalized Unified Formulation for the analysis of composite structures. Compos. Struct., 142: 187-199. [https://doi.org/10.1016/j.compstruct.2016.01.087].
6. Wang B, Min H Q and Qu T (2023) Damping characteristics and sound transmission loss of finite composite plates with frequency dependent constrained viscoelastic interlayer. Mech. Adv. Mater. Struct.[https://doi.org/10.1080/15376494.2023.2253789]
7. Zhang G S, Zheng H, Mi Y Z, and Li F (2024). Soundbox-based sound insulation measurement of composite panels with viscoelastic damping. Int. J. Mech. Sci., 283.[https://doi.org/10.1016/j.ijmecsci.2024.109663].
8. Li Y S, Liu B L, Li S, and Shi H W (2024). Vibro-acoustic response and sound transmission loss of sandwich plates with tunable poisson's ratio core in a hygrothermal environment. "Eur. J. Mech. A-Solids, 106.[https://doi.org/10.1016/j.euromechsol.2024.105281].
9. DavidA (1988) Engineering noise control : theory and practice. Unwin Hyman.
10. Mahjoob M J, Mohammadi N, and Malakooti S (2009) An investigation into the acoustic insulation of triple-layered panels containing newtonian fluids: theory and experiment. Appl. Acoust., 70: 165-171.[https://doi.org/10.1016/j.apacoust.2007.12.002].
11. Zhou R and M.J. Crocker (2010) Boundary element analyses for sound transmission loss of panels. J. Acoust. Soc. Am., 127: 829-840.[https://doi.org/10.1121/1.3273885].
12. Lee J H, and Ih J G (2004). Significance of resonant sound transmission in finite single partitions. J. Sound Vib., 277, 881-893.[https://doi.org/10.1016/j.jsv.2003.09.023].